Available online at www.sciencedirect.com
ScienceDirect
Journal of the Franklin Institute 348 (2011) 2191–2215
Journal of The Franklin Institute
www.elsevier.com/locate/jfranklin

Design of optimal strictly positive real controllers using numerical optimization for the control of flexible robotic systems

James Richard Forbes[a,*], Christopher John Damaren[b]

[a]Department of Mechanical Engineering, McGill University, 817 Sherbrooke Street West, Montreal, Quebec, Canada H3A 2K6

[b]University of Toronto Institute for Aerospace Studies, 4925 Dufferin Street, Toronto, Ontario, Canada M3H 5T6

Received 30 September 2009; received in revised form 1 June 2011; accepted 13 June 2011
Available online 19 July 2011

Abstract

The design of optimal strictly positive real (SPR) controllers using numerical optimization is considered. We focus on how to parameterize the SPR controllers being optimized and the effect of parameterization. Minimization of the closed-loop $\mathcal{H}_2$-norm is the optimization objective function. Various single-input single-output and multi-input multi-output controller parameterizations using transfer functions/matrices and state–space equations are considered. Depending on the controller form, constraints are enforced (i) using simple inequalities guaranteeing SPRness, (ii) in the frequency domain or, (iii) by implementing the Kalman–Yakubovich–Popov Lemma. None of the parameterizations we consider foster an observer-based controller structure. Simulated control of a single-link and a two-link flexible manipulators demonstrates the effectiveness of our proposed controller optimization formulations.

1. Introduction

The passivity theorem is one of the most celebrated results in input–output systems theory. In general, a passive system is one that does not generate energy and a very strictly passive system is one that dissipates energy. The passivity theorem states that a passive system and a very strictly passive system connected in a negative-feedback loop are input–output stable [1]. This is

*Corresponding author.
E-mail addresses: james.richard.forbes@mcgill.ca (J.R. Forbes), damaren@utias.utoronto.ca (C.J. Damaren).

0016-0032/$32.00 © 2011 The Franklin Institute. Published by Elsevier Ltd. All rights reserved.
doi:10.1016/j.jfranklin.2011.06.013

an extremely powerful statement in the context of nonlinear control; stability of a nonlinear yet passive plant is guaranteed via control in the form of a very strictly passive operator.

In the context of passive mechanical systems, inputs are forces and outputs are rates such as velocity. Flexible structures possess a large number of vibration modes, and in robotics applications have dynamics that are nonlinear. Flexible robotic manipulators are known to be passive via collocation of the joint torques and the angular velocity sensors, that is when the input–output map is between the joint torques and joint angular velocities. The passivity property for these collocated systems is independent of the system mass, stiffness, and modeled vibration modes. The noncollocated map between joint torques and end-tip velocity of a manipulator is not passive, but the map between a modified set of joint torques and a modified output, known as the μ-tip rate, has been shown to be passive, thus facilitating passivity-based control of the μ-tip rate [2].

Passive and very strictly passive systems that are linear and time-invariant (LTI) are closely related to positive real (PR) and strictly positive real (SPR) transfer functions or matrices [3]. The robust stability of nonlinear flexible robotic manipulators is assured via the passivity theorem when the controllers employed are SPR. In particular, spillover instabilities are avoided. In light of this important stability result, many authors have attempted to formulate rate controllers such that they are SPR. Benhabib et al. [4] suggested the use of SPR rate controllers to control large space structures where the controllers considered were not observer-based. Similarly, McLaren and Slater [5] investigated implementing positive real LQG controllers for the control of large space structures. Lozano-Leal and Joshi [6] investigated the design of LQG controllers, constraining the LQG weight matrices such that the resultant optimal controllers remain SPR. Haddad et al. [7] extend the work of Lozano-Leal and Joshi [6] to include an $\mathcal{H}_\infty$ performance bound on the closed-loop, again by constraining the appropriate weighting matrices.

The use of numerical optimization algorithms to find optimal SPR controllers has been considered in various papers. In Germoel and Gapsik [8] the design of observer-based SPR compensators using convex numerical optimization was considered. Using linear matrix inequality (LMI) constraints, the $\mathcal{H}_2$-optimal control problem was retooled to yield SPR controllers. The controllers were full order, meaning that the controllers and the plant model to be controlled have the same number of system states. Shimomura and Pullen [9] extended the work of Germoel and Gapsik [8], considering the use of iterative algorithms that overcome bilinear matrix inequality issues within the optimal SPR optimization formulation. Again, the resultant controllers were observer-based and full order.

In both Germoel and Gapsik [8] and Shimomura and Pullen [9] the observer gains were those found via the solution to the unconstrained $\mathcal{H}_2$-optimal control problem. In Damaren [10], the optimization of single-input single-output SPR controllers of varying order was considered. The SPR controllers were not full order, nor observer-based compensators. Simple inequality constraints in the frequency domain via a transformation from the s-domain to the z-domain guaranteed SPRness. In Damaren et al. [11], optimal SPR controllers that approximate a given observer-based, full order controller were found by solving a quadratic programming problem with linear inequality constraints. In Henrion [12] a method using LMIs is presented whereby a transfer function can be designed to be robustly rendered SPR given a Hurwitz denominator polynomial.

Other than the work of Benhabib et al. [4] and Damaren [10], the existing SPR design schemes (that is, optimal design schemes) yield controllers that are observer-based, and thus have the same order as the plant. It remains an open question as to whether or not the optimal SPR controller that solves the $\mathcal{H}_2$ control problem is observer-based, or even should be the same

order as the plant being controlled. Because unconstrained $\mathcal{H}_2$-optimal controllers are observer-based, it does not mean that optimal SPR controllers must be observer-based. Also, if the dimension of the plant is large (as is the case with flexible robotic manipulators and structures), having a controller that is lower order yet still optimal is desirable. With this in mind, we will explore various controller parameterizations of various orders that are not observer-based, constrain the controllers to be SPR (in different ways, depending on the parameterization at hand), and optimize the controllers numerically by minimizing the closed-loop $\mathcal{H}_2$-norm of the system. One of the questions we hope to shed light on is that of controller order. Additionally, the existing literature often considers the control of a pinned–pinned Euler–Bernoulli beam [7–10]. In our work, we consider the tip control of single- and two-link flexible robotic manipulators. Recall that the SPR controllers we parameterize and optimize will be rate (velocity) controllers. To realize position control, the manipulators must also be compensated by position (i.e., proportional) control. We will include the proportional control gain as a design variable, which is equivalent to optimally designing the rigid-body mode of the plant in conjunction with the rate controller.

The outline of the paper is as follows: in the next section we will briefly review the conditions which ensure that a system is SPR. We then consider flexible manipulator modeling and tip-based control. Both two- and single-link flexible manipulator models will be considered. In Section 4 we will state our numerical optimization objective function. Although we will consider various controller parameterizations and constraint methods in this paper, we will always be minimizing the closed-loop $\mathcal{H}_2$-norm of the system. We then move onto the main contributions of the paper. In Section 5 we consider three different SISO controller parameterizations, as well as ways to constrain the controllers based on the parameterizations. In Section 6 we then modify the parameterizations (and constraints) for MIMO controller design. Simulated control of the single- and two-link flexible manipulators is included. We close with a discussion and final remarks.

2. Strictly positive real transfer functions and matrices

Definition 1 (*SPR transfer functions*). A real, rational, strictly proper transfer function, $g(s)$, of the complex variable s is SPR if [13]

1. $g(s)$ is real for all real s and $g(s)$ is analytic $Re\{s\} \geq 0$,
2. $Re\{g(j\omega)\} > 0 \ \forall \omega \in (-\infty, \infty)$,
3. $\lim_{\omega \to \infty} \omega^2 Re\{g(j\omega)\} > 0$.

Definition 2 (*SPR transfer matrices and the Kalman–Yakubovich–Popov (KYP) lemma*). A real, rational, strictly proper transfer matrix, $\mathbf{G}(s)$, of the complex variable s is SPR if [14,15]

1. $\mathbf{G}(s)$ is real for all real s and all elements of $\mathbf{G}(s)$ are analytic in $Re\{s\} \geq 0$,
2. $\mathbf{G}(j\omega) + \mathbf{G}^{\mathsf{H}}(j\omega) > \mathbf{0} \ \forall \omega \in (-\infty, \infty)$,
3. $\lim_{\omega \to \infty} \omega^2 \{\mathbf{G}(j\omega) + \mathbf{G}^{\mathsf{H}}(j\omega)\} > \mathbf{0}$.

Additionally, if $\mathbf{G}(s) = \mathbf{C}_c(s\mathbf{I} - \mathbf{A}_c)^{-1}\mathbf{B}_c$ where $\{\mathbf{A}_c, \mathbf{B}_c, \mathbf{C}_c\}$ is a minimal realization, and there exist $\mathbf{P}_c = \mathbf{P}_c^{\mathsf{T}} > \mathbf{0}$ and $\mathbf{Q}_c = \mathbf{Q}_c^{\mathsf{T}} > \mathbf{0}$ such that [16,17]

$$\mathbf{P}_c\mathbf{A}_c + \mathbf{A}_c^{\mathsf{T}}\mathbf{P}_c = -\mathbf{Q}_c \tag{1a}$$

$$\mathbf{P}_c\mathbf{B}_c = \mathbf{C}_c^{\mathsf{T}} \tag{1b}$$

then $\mathbf{G}(s)$ is SPR.

3. Flexible manipulator modeling

We are interested in controlling (using optimal SPR controllers) a single-link manipulator and a two-link manipulator that carry large payloads. Both manipulators possess flexible links, as shown in Fig. 1. We will briefly review the differential equations describing the dynamics of each; for a more complete derivation of the dynamics of flexible systems, refer to Damaren [2], Damaren and Sharf [18].

3.1. Two-link manipulator modeling

The nonlinear dynamic equations of motion for a two-link flexible robotic manipulator carrying a large payload (and in general any flexible robotic manipulator with more than two links) can be written as

$$\mathbf{M}(\boldsymbol{\theta},\mathbf{q}_e)\ddot{\mathbf{q}} + \mathbf{K}\mathbf{q} = \hat{\mathbf{B}}(\boldsymbol{\tau} + \mathbf{w}_1) + \mathbf{f}_{non}(\boldsymbol{\theta},\mathbf{q}_e,\dot{\boldsymbol{\theta}},\dot{\mathbf{q}}_e)$$

where $\mathbf{M} = \mathbf{M}^{\mathsf{T}} > \mathbf{0}$ and $\mathbf{K} = \mathbf{K}^{\mathsf{T}} \geq \mathbf{0}$ are the mass and stiffness matrices, $\hat{\mathbf{B}} = [\mathbf{I}\ \mathbf{0}]^{\mathsf{T}}$, and $\mathbf{f}_{non} = [\mathbf{f}_{non,\theta}^{\mathsf{T}}\ \mathbf{f}_{non,e}^{\mathsf{T}}]^{\mathsf{T}}$ captures the nonlinear inertia forces stemming from centrifugal and Coriolis accelerations. The generalized coordinates, joint torques, and disturbance torques are $\mathbf{q} = [\boldsymbol{\theta}^{\mathsf{T}}\ \mathbf{q}_e^{\mathsf{T}}]^{\mathsf{T}}$, $\boldsymbol{\tau} = [\tau_1\ \tau_2]^{\mathsf{T}}$, and $\mathbf{w}_1$, respectively, for the two-link model being considered, where $\boldsymbol{\theta} = [\theta_1\ \theta_2]^{\mathsf{T}}$ are the columnized joint angles, and $\mathbf{q}_e$ are the columnized elastic coordinates associated with discretization of flexible links [19].

We will be concerned with the control of the robot tip velocity $\dot{\boldsymbol{\rho}}_{\mu=1} = [v_x\ v_y]^{\mathsf{T}}$ where

$$\dot{\boldsymbol{\rho}}_{\mu} = \mathbf{J}_{\theta}(\boldsymbol{\theta},\mathbf{q}_e)\dot{\boldsymbol{\theta}} + \mu\mathbf{J}_e(\boldsymbol{\theta},\mathbf{q}_e)\dot{\mathbf{q}}_e$$

Here, $\mathbf{J}_{\theta}$ is the rigid Jacobian and $\mathbf{J}_{\theta}(\boldsymbol{\theta},\mathbf{0})$ maps joint rates to spatial velocities if the manipulator was rigid, and $\mathbf{J}_e$ is the elastic Jacobian that maps the elastic rates to the tip rate as if the joints were locked. The mapping between the joint torques and the actual tip rate is not passive. In Damaren [20] it was shown that for manipulators carrying large payloads the modified input–output mapping between $\mathbf{u} = \mathbf{J}_{\theta}^{-\mathsf{T}}\boldsymbol{\tau}$ and the μ-tip rate,

$$\dot{\boldsymbol{\rho}}_{\mu} = \mathbf{J}_{\theta}(\boldsymbol{\theta},\mathbf{q}_e)\dot{\boldsymbol{\theta}} + \mu\mathbf{J}_e(\boldsymbol{\theta},\mathbf{q}_e)\dot{\mathbf{q}}_e = \mu\dot{\boldsymbol{\rho}}_{\mu=1} + (1-\mu)\mathbf{J}_{\theta}(\boldsymbol{\theta},\mathbf{q}_e)\dot{\boldsymbol{\theta}} \tag{2}$$

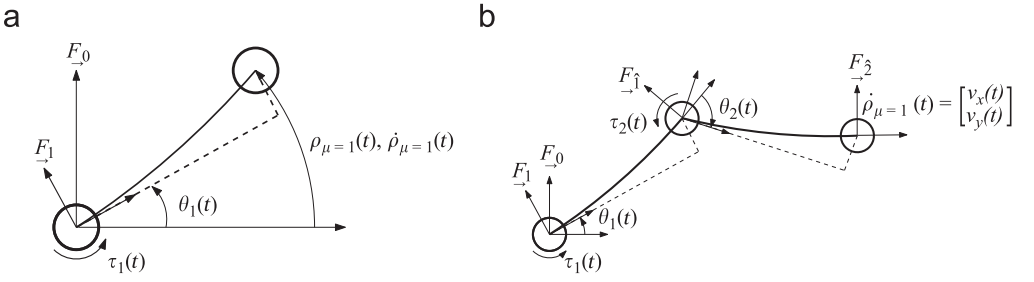

Fig. 1. Single-link and two-link flexible manipulators.

is passive when $0 \leq \mu < 1$. This modified input–output mapping is necessary in order to implement the passivity theorem. The true-tip rate is captured by $\mu = 1$, which as previously mentioned, when combined with $\mathbf{u}$ does not represent a passive map. In general, μ should be picked to be as close to one as possible, thus having $\dot{\boldsymbol{\rho}}_\mu$ closely resemble the true-tip velocity. The numerical simulation to be presented in future sections will use $\mu = 0.8$, thus ensuring that the mapping $\mathbf{u} \to \dot{\boldsymbol{\rho}}_\mu$ is passive.

In the future, we not only implement rate control, but also position control in the form of proportional control. From the definition of $\dot{\boldsymbol{\rho}}_\mu$ in Eq. (2), by assuming $\mathbf{J}_\theta(\boldsymbol{\theta}, \mathbf{q}_e) = \mathbf{J}_\theta(\boldsymbol{\theta}, \mathbf{0})$ we can approximate $\boldsymbol{\rho}_\mu$ as $\boldsymbol{\rho}_\mu \doteq \mu \boldsymbol{\rho}_{\mu=1} + (1-\mu)\boldsymbol{F}_r(\boldsymbol{\theta})$. $\boldsymbol{F}_r(\boldsymbol{\theta})$ is the rigid forward kinematics map, as defined in Damaren [19].

Our control objective is to have the two-link manipulator previously discussed follow a pre-specified tip trajectory, $\boldsymbol{\rho}_d$. We can define $\boldsymbol{\rho}_d$ and $\dot{\boldsymbol{\rho}}_d$ based on an equivalent rigid robot joint trajectory, mapped through the forward kinematics, $\boldsymbol{\rho}_d = \boldsymbol{F}_r(\boldsymbol{\theta}_d)$. In future sections we will employ the following desired joint trajectory in order to calculate $\boldsymbol{\rho}_d$ and $\dot{\boldsymbol{\rho}}_d$:

$$\boldsymbol{\theta}_d = \left[10\left(\frac{t-t_a}{t_b-t_a}\right)^3 - 15\left(\frac{t-t_a}{t_b-t_a}\right)^4 + 6\left(\frac{t-t_a}{t_b-t_a}\right)^5 \right](\boldsymbol{\theta}_b - \boldsymbol{\theta}_a) + \boldsymbol{\theta}_a \tag{3}$$

where $\boldsymbol{\theta}_a$ is the initial joint configuration, $\boldsymbol{\theta}_b$ is the final joint configuration, and $t_b - t_a$ is the time allotted for the manipulator to move from joint configuration $\boldsymbol{\theta}_a$ to joint configuration $\boldsymbol{\theta}_b$. The manipulator is initially at rest at $\boldsymbol{\theta}_a$, and is to stop at $\boldsymbol{\theta}_b$. It is important to realize that this is only used to provide a smooth desired tip trajectory, $\boldsymbol{\rho}_d$ [11]. It is not expected that the joint angles will follow the desired joint trajectory.

In most practical applications control would be a combination of feedforward and feedback control, $\boldsymbol{\tau} = \boldsymbol{\tau}_{ff} + \boldsymbol{\tau}_{fb}$. Feedforward control is essentially a method by which a portion of the nonlinear dynamics present in a system are canceled out. In the case of a two-link flexible manipulator carrying a massive payload, an effective feedforward is simply the rigid inverse dynamics of the system:

$$\boldsymbol{\tau}_{ff} = \mathbf{M}_{\theta\theta}(\boldsymbol{\theta}_d, \mathbf{0})\ddot{\boldsymbol{\theta}}_d - \mathbf{f}_{non,\theta_d}$$

where $\mathbf{f}_{non,\theta_d}$ is the joint angle partition of $\mathbf{f}_{non}$ evaluated at the desired trajectory. Our feedback control will be a combination of position and rate control:

$$\boldsymbol{\tau}_{fb} = -\mathbf{J}_\theta^{\mathsf{T}}[\mathbf{K}_p(\boldsymbol{\rho}_\mu - \boldsymbol{\rho}_d) + \boldsymbol{G}(\dot{\boldsymbol{\rho}}_\mu - \dot{\boldsymbol{\rho}}_d)]$$

where $\mathbf{K}_p$ represent proportional control and $\boldsymbol{G}$ is a system operator representing a linear SPR controller with transfer matrix $\mathbf{G}(s)$. Our two-link manipulator simulations presented in future sections will employ both feedforward and feedback control.

3.2. Single-link manipulator modeling

The linear equations of motion for a single-link flexible robotic manipulator carrying a large payload can be written as

$$\mathbf{M}\ddot{\mathbf{q}} + \mathbf{K}\mathbf{q} = \hat{\mathbf{b}}(\tau_1 + w_1)$$

where $\mathbf{M} = \mathbf{M}^{\mathsf{T}} > \mathbf{0}$ and $\mathbf{K} = \mathbf{K}^{\mathsf{T}} \geq \mathbf{0}$ are the mass and stiffness matrices, and $\hat{\mathbf{b}} = [1\ \mathbf{0}]^{\mathsf{T}}$. The generalized coordinates, joint torque, and disturbance torque are $\mathbf{q} = [\theta_1\ \mathbf{q}_e^{\mathsf{T}}]^{\mathsf{T}}$, τ_1, and w_1, respectively, where $\mathbf{q}_e$ are the columnized elastic coordinates.

As in the two-link case, we are concerned with the μ-tip rate:

$$\dot{\rho}_\mu = J_\theta \dot{\theta}_1 + \mu \mathbf{J}_e \dot{\mathbf{q}}_e$$

where $0 \leq \mu < 1$. The input–output map between $u = J_\theta^{-1}\tau_1$ and $y = \dot{\rho}_\mu$ is passive for large payloads. The numerical simulations presented in future sections will use $\mu = 0.8$, again ensuring a passive map between u and y. When $\mu = 1$, the output is the true-tip rate, but the map between u and $\dot{\rho}_{\mu=1}$ is not passive (that is, the transfer function is not PR).

Like the two-link manipulator, the feedback controller will be composed of position and rate control. Unlike the two-link case, our control objective will be as that of regulation, rather than tracking; the single-link manipulator tip position and velocity will be regulated to zero.

4. Optimization objective function

Both the single-link and linearized two-link manipulator differential equations can be cast into a general state–space form:

$$\begin{aligned}\dot{\mathbf{x}} &= \mathbf{A}\mathbf{x} + \mathbf{B}_1\mathbf{w} + \mathbf{B}_2\mathbf{u}\\ \mathbf{z} &= \mathbf{C}_1\mathbf{x} + \mathbf{D}_{12}\mathbf{u}\\ \mathbf{y} &= \mathbf{C}_2\mathbf{x} + \mathbf{D}_{21}\mathbf{w}\end{aligned} \tag{4}$$

where $\mathbf{x} \in \mathbb{R}^n$ are the system states (composed of the number of joint angles, the elastic coordinates, and both their rates), $\mathbf{u} \in \mathbb{R}^m$ is the control input, $\mathbf{y} \in \mathbb{R}^m$ are the noisy system measurements (that being $\dot{\rho}_\mu + w_2$ in the SISO case or $\dot{\boldsymbol{\rho}}_\mu + \mathbf{w}_2$ in the MIMO case), $\mathbf{z} \in \mathbb{R}^q$ is the regulated output (that being the actual tip position and rate, $\rho_{\mu=1}$ and $\dot{\rho}_{\mu=1}$ or $\boldsymbol{\rho}_{\mu=1}$ and $\dot{\boldsymbol{\rho}}_{\mu=1}$) and $\mathbf{w} = [\mathbf{w}_1^\mathsf{T}\ \mathbf{w}_2^\mathsf{T}]^\mathsf{T}$, $\mathbf{w} \in \mathbb{R}^l$ represents system disturbances/noise. We will assume that:

1. $(\mathbf{A},\mathbf{B}_1)$ is controllable and $(\mathbf{C}_1,\mathbf{A})$ is observable;
2. $(\mathbf{A},\mathbf{B}_2)$ is controllable and $(\mathbf{C}_2,\mathbf{A})$ is observable;
3. $\mathbf{D}_{12}^\mathsf{T}\mathbf{C}_1 = \mathbf{0}$ and $\mathbf{D}_{12}^\mathsf{T}\mathbf{D}_{12} > \mathbf{0}$;
4. $\mathbf{D}_{21}\mathbf{B}_1^\mathsf{T} = \mathbf{0}$ and $\mathbf{D}_{21}\mathbf{D}_{21}^\mathsf{T} > \mathbf{0}$.

Consider a general SPR controller $\mathbf{u} = -\boldsymbol{G}\mathbf{y}$ in state–space form:

$$\begin{aligned}\dot{\mathbf{x}}_c &= \mathbf{A}_c\mathbf{x}_c + \mathbf{B}_c\mathbf{y}\\ \mathbf{u} &= -\mathbf{C}_c\mathbf{x}_c\end{aligned}$$

Combining the (linearized) plant and controller yields the closed-loop system dynamics:

$$\begin{bmatrix}\dot{\mathbf{x}}\\ \dot{\mathbf{x}}_c\end{bmatrix} = \underbrace{\begin{bmatrix}\mathbf{A} & -\mathbf{B}_2\mathbf{C}_c\\ \mathbf{B}_c\mathbf{C}_2 & \mathbf{A}_c\end{bmatrix}}_{\mathbf{A}_{zw}}\underbrace{\begin{bmatrix}\mathbf{x}\\ \mathbf{x}_c\end{bmatrix}}_{\mathbf{x}_{zw}} + \underbrace{\begin{bmatrix}\mathbf{B}_1\\ \mathbf{B}_c\mathbf{D}_{21}\end{bmatrix}}_{\mathbf{B}_{zw}}\mathbf{w}$$

$$\mathbf{z} = \underbrace{\begin{bmatrix}\mathbf{C}_1 & -\mathbf{D}_{12}\mathbf{C}_c\end{bmatrix}}_{\mathbf{C}_{zw}}\begin{bmatrix}\mathbf{x}\\ \mathbf{x}_c\end{bmatrix}$$

Our optimization objective function will be *minimization of the closed-loop* $\mathcal{H}_2$-norm *of the (linearized) system while varying design variables associated with the parameterization of an SPR controller*. The closed-loop $\mathcal{H}_2$-norm can be calculated via

$$\mathcal{J}_2 = \sqrt{\text{tr } \mathbf{B}_{zw}^{\mathsf{T}} \mathbf{P} \mathbf{B}_{zw}}$$

The matrix $\mathbf{P} = \mathbf{P}^{\mathsf{T}} > \mathbf{0}$ is found by solving the Lyapunov equation

$$\mathbf{P}\mathbf{A}_{zw} + \mathbf{A}_{zw}^{\mathsf{T}} \mathbf{P} = -\mathbf{C}_{zw}^{\mathsf{T}} \mathbf{C}_{zw}$$

The optimization design variables and constraints (that is, the constraints enforcing the controller to be SPR) are parameterization dependent, and will be discussed in the following sections in the SISO and MIMO cases. Also, note that we will be altering the controller parameterization; the performance index remains static (i.e., the weights $\mathbf{B}_1$, $\mathbf{C}_1$, $\mathbf{D}_{12}$, $\mathbf{D}_{21}$ do not change). In fact, the performance index we have chosen yields a traditional $\mathcal{H}_2$ controller that is not SPR, and hence not robust to mass and stiffness perturbations.

Although we are concerned with the design of rate controllers which will be constrained to be SPR, prior to designing such a controller the plant must be prewrapped with position-based proportional control. This corresponds to feeding back the μ-tip position, ρ_μ or $\boldsymbol{\rho}_\mu$, and does not alter the passivity of the system. The proportional control gain, $K_p > 0$ in the SISO case, and $\mathbf{K}_p = \mathbf{K}_p^{\mathsf{T}} > \mathbf{0}$ in the MIMO case, will be included as design variables during the optimization process.

There are many numerical optimization methods available, however we elect to use a Sequential Quadratic Programming (SQP) formulation. For a detailed discussion of an SQP optimizer, interested readers may consult [21]. Briefly, an SQP method is a gradient-based optimization procedure that utilizes the Karush–Kuhn–Tucker (KKT) conditions to ensure that both the optimum solution has been found, and the constraints have been satisfied.

Because an SQP optimizer is gradient-based, there is no guarantee that the optimization will converge to a global optimum. Therefore, the solutions presented in the forthcoming sections are not necessarily global optima, but rather local optima which are dependent on the initial conditions of the numerical optimization algorithm.

5. Optimization of SISO SPR controllers to control a single-link flexible manipulator

In this section, we will explore different approaches to SISO controller parameterization; designing the form of the controller, specifying the design variables, and enforcing the constraints. As previously mentioned, the control objective is regulation of the tip position and rate to zero. All simulations to follow will use $[\rho(0)_{\mu=1} \ \dot{\rho}(0)_{\mu=1}]^{\mathsf{T}} = \left[(\pi/4) \ 1\right]^{\mathsf{T}}$ (m,m/s) as initial conditions. The physical values of the single-link manipulator length, mass, tip-mass, hub inertia, etc. used during optimization and simulation are given in Table 1.

5.1. Third-order SPR controller with deterministic constraints

Marquez and Damaren [22] have developed a formulation such that given a strictly proper transfer function with a denominator polynomial that is Hurwitz, necessary and sufficient conditions are formulated that, when met, will always yield a numerator polynomial that creates an SPR transfer function. The formulation allows the numerator

Table 1
Single-link manipulator physical properties.

Length	L	1 (m)
Link mass	m	1 (kg)
Modulus of elasticity	E	70×10^9 (Pa)
Link height	h	75 (mm)
Link base width	w	2 (mm)
Link second moment of area	$I = \frac{1}{12}hw^3$	5×10^{-11} (m^4)
Hub mass	m_{hub}	1 (kg)
Hub mass moment of inertia	J_{hub}	3.125×10^{-4} (kg m^2)
Tip mass	m_{tip}	1.5 (kg)

polynomial to be expressed as a function of the denominator polynomial coefficients and three additional constrained variables: k_1, k_2, and k_3 (in the third-order case).

Consider a third-order controller; the controller input is $\dot{\rho}_\mu$ (not the tip position, rather the μ-tip rate), and the output is the modified joint torque, $u = J_\theta^{-1}\tau_1$. We will assume that the denominator polynomial renders the transfer function Hurwitz, and in general this is straightforward to impose as a numerical optimization constraint. A simple Hurwitz or Routh–Hurwitz check will determine if the poles of the transfer function

$$g(s) = \mathbf{C}_c(s\mathbf{I}-\mathbf{A}_c)^{-1}\mathbf{B}_c = \frac{n_2 s^2 + n_1 s + n_0}{s^3 + as^2 + bs + c} \tag{5}$$

are in the open left-half complex plane. Following the developments of Marquez and Damaren [22], the numerator polynomial coefficients are defined as functions of k_1, k_2 and k_3 as follows:

$$n_2 = \frac{bck_1 + ck_2 + ak_3}{abc-c^2}, \quad n_1 = \frac{c^2k_1 + ack_2 + a^2k_3}{abc-c^2}, \quad n_0 = \frac{k_3}{c}$$

In order for the controller to be SPR (and thus satisfy Definition 2.1) the following inequalities must be met:

$$k_1 \geq 0, \quad k_2 > -2\sqrt{k_1k_3}, \quad k_3 > 0.$$

Given the above SISO controller form and parameterization above, the numerical optimization problem is posed as follows:

Design variables: $\mathbf{x} = [a\ b\ c\ k_1\ k_2\ k_3\ K_p]$;

Constraints: $Re\{\lambda_i(\mathbf{A}_c)\} < 0$ for $i = 1, \ldots, n$, $k_1 \geq 0$, $k_2 > -2\sqrt{k_1k_3}$, $k_3 > 0$, $K_p > 0$;

Objective function: Closed-loop $\mathcal{H}_2$-norm: $\mathcal{J}_2 = \sqrt{\text{tr } \mathbf{B}_{zw}^{\mathsf{T}}\mathbf{P}\mathbf{B}_{zw}}$.

Notice that the proportional control gain is a design variable as well. Additionally, we are optimizing an order three transfer function, and the controller is not constrained to be observer-based.

5.1.1. Optimization results

The objective function was minimized to a value of $\mathcal{J}_2 = 2.8293$. The convergence tolerance was set to 1×10^{-8}. The Bode diagram of the optimized SPR controller is shown in Fig. 2. The simulated system response of the true-tip position and velocity is shown in Fig. 3. Note, although we are measuring and feeding back the μ-tip position and velocity

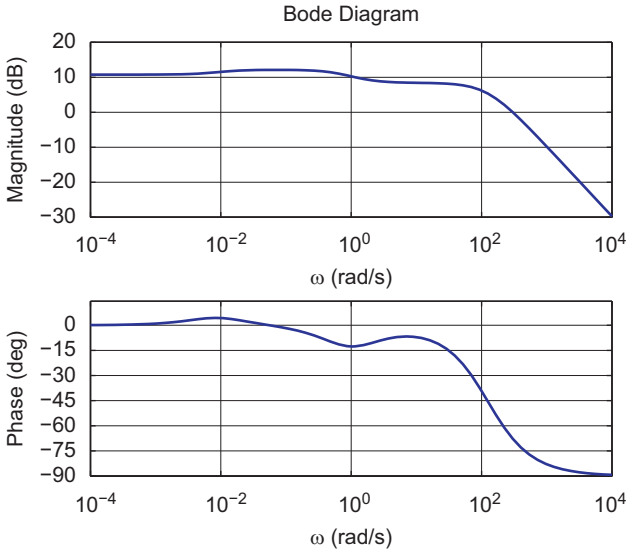

Fig. 2. Bode diagram of third-order SPR controller.

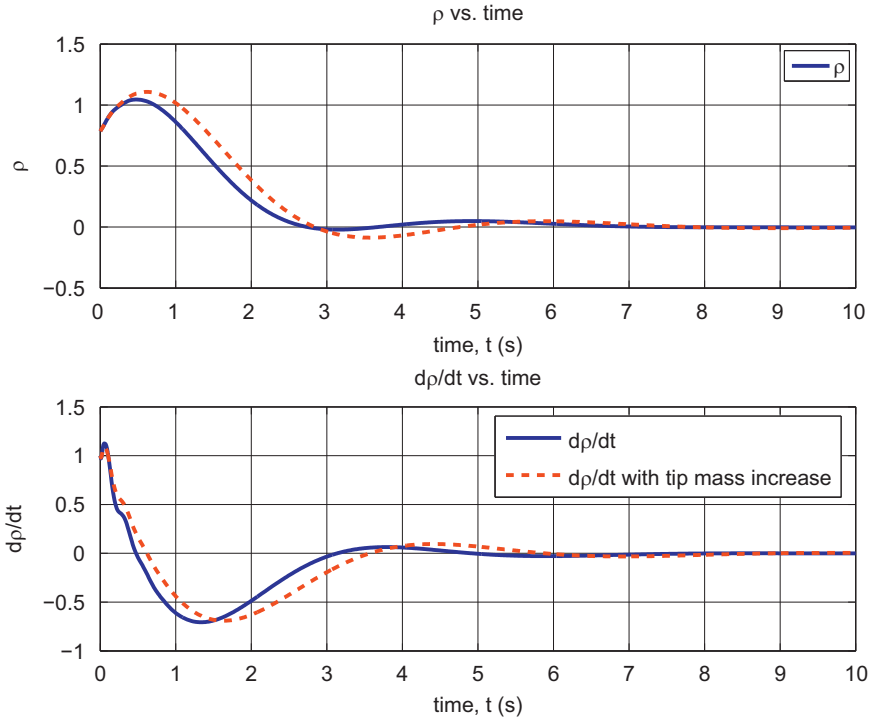

Fig. 3. System response using optimal third-order SPR controller, with and without tip mass increase.

(to the proportional and SPR controllers, respectively), we are interested in the true-tip position and velocity response.

Notice in Fig. 2 that the compensator has high gain at low frequency, and subsequently rolls off at high frequency. Such a response is desirable in practice for two reasons. First, high gain at low frequency realizes excellent tracking and regulation. Second, roll off of the controller at high frequency ensures that high frequency disturbances and signal noise are rejected.

Referring to Fig. 3, the SPR controller clearly regulates the manipulator tip position and velocity to zero. In the bottom portion of Fig. 3, we can see that at approximately 0.25 s the tip is vibrating slightly, but the vibration is quickly suppressed, and then the manipulator smoothly approaches the desired position. There is some, but still a minimal amount of overshoot. The manipulator comes to rest after approximately 7 s.

Recall that we seek to optimally design SPR controllers because they are robust to modeling errors associated with, for example, the flexible manipulator mass distribution. In Fig. 3 we also show the system response when the tip mass has been increased 1.5 times. This change will alter the natural frequencies of the system, and can be considered a rather large modeling perturbation. From Fig. 3 we can clearly see that the system is regulated to zero, although there is a slight increase in the amount of overshoot and settling time.

5.2. Variable-order SPR controller with frequency domain constraints

In the previous section we optimized a third-order controller. We want to be able to optimize a controller that is strictly proper (so that the controller rolls off at high frequency), but of any order. Consider the following controller parameterization, often called a "Ritz" parameterization:

$$g(s) = \sum_{n=1}^{N} h_n \frac{(s-a)^{n-1}}{(s+a)^n} \tag{6}$$

where N is a finite positive integer, $a>0$, and $h_n \in \mathbb{R}$. Similar controller parameterizations can be found in Polak and Salcudean [23], Hu et al. [24], Boyd and Barratt [25]; in particular, the parameterization in Eq. (6) was also used in Damaren [10] where a was held fixed and equal to one.

Within a numerical optimization setting, the controller parameterization given in Eq. (6) is attractive for many reasons. First, when a is held fixed, the transfer function $g(s)$ is a linear function of the coefficients h_n. Second, the expansion in Eq. (6) is dense in $\mathcal{H}_2$ as $N \to \infty$, which is to say, any real rational strictly proper transfer function in $\mathcal{H}_2$ can be uniformly approximated arbitrarily close by using the expansion in Eq. (6).

Using the parameterization presented in Eq. (6), a controller will be optimized in the following way. First, a controller of order n will be optimized, then the design space will be expanded and a controller of order $n+1$ is optimized. Consider the simplified illustrations in Fig. 4: a controller of order one (denominator polynomial of order 1) will be optimized and some optimal h_1, a, and K_p values will be found. Next, a controller of order two will be optimized; the initial conditions for this next optimization will be the optimal values of h_1, a, and K_p from the previous optimization run and h_2 will be approximately zero (1×10^{-14}). This ensures that the optimizer is "starting" with a feasible solution and then finding the optimal solution in the new design space.

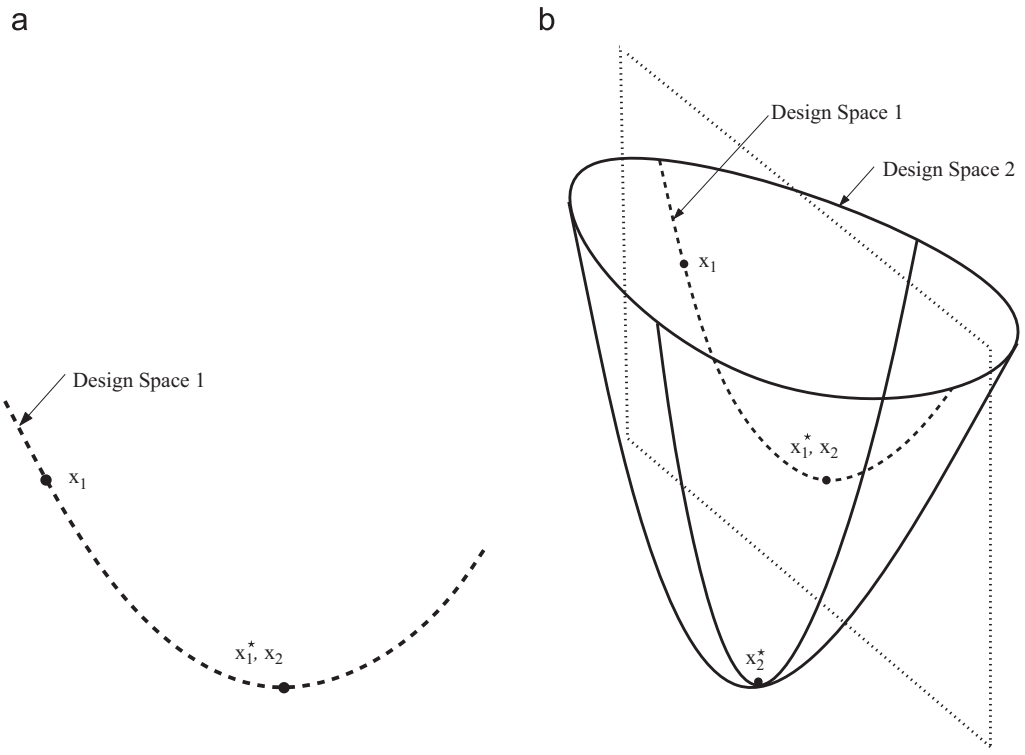

Fig. 4. Design space expansion. (a) Design space of controller with $n=1$. (b) Design space of controller with $n=2$.

Let us now return to Definition 2.1, the frequency domain requirements for a transfer function to be SPR. The first of the SPR criteria is straightforward to impose as a numerical optimization constraint. As mentioned in Section 5.1, a Hurwitz or Routh–Hurwitz check will determine whether the poles of the transfer function (of any order) are in the open left-half complex plane. The second SPR condition, that is $Re\{g(j\omega)\}>0$, will be checked at N logarithmically spaced points within each decade over $\omega \in (0,\infty)$. The last of the SPR criteria is not specifically enforced as a constraint during the optimization. One might think that this is a significant problem, however it is not, for it has been proven that a weak SPR transfer function (i.e., condition 3 is not satisfied) can stabilize a passive system. Additionally, it is highly unlikely that the optimal values of the design variables would render the transfer function weak SPR.

Given the variable-order SISO controller parameterization, the numerical optimization problem is posed as follows:

Design variables: $\mathbf{x}=[h_1\ h_2\ \ldots\ h_n\ a\ K_p]$;

Constraints: $Re\{\lambda_i(\mathbf{A}_c)\}<0$ for $i=1,\ldots,n$, $Re\{g(j\omega)\}>0\ \forall\omega\in(0,\infty)$;

Objective function: Closed-loop $\mathcal{H}_2$-norm: $\mathcal{J}_2=\sqrt{\text{tr}\ \mathbf{B}_{zw}^{\mathsf{T}}\mathbf{P}\mathbf{B}_{zw}}$.

5.2.1. Optimization results

The optimization was first started with a controller of order one (i.e., $g(s)=h_1/(s+a)$) and the order was increased to a fifth order controller. The final value of the objective

function for the optimized fifth-order controller was $\mathcal{J}_2 = 2.7925$. The convergence tolerance was set to 1×10^{-8}. The optimization results are tabulated in Table 2.

The evolution of the controller frequency response and the closed-loop system responses as the controller order is increased and optimized from $n=1$ to 5 is quite interesting. From the Bode diagrams in Fig. 5 we can see how the controller gradually morphs from a simple low pass filter to a more complicated and better controller. The controller is "better" in that, when looking at the system response in Fig. 6, there is less overshoot and the settling time decreases as the controller order increases and is optimized. What is interesting is that the optimization formulation has no direct constraint on the tolerable rise time, amount of overshoot, settling time, etc., but at the same time the system response improves as the controller increases in complexity and is optimized.

Table 2
Variable-order SISO SPR controller optimization evolution.

n	$\mathcal{J}_2$	K_p	a	h_1	h_2	h_3	h_4	h_5
1	2.9226	2.1565	67.5816	147.0903	–	–	–	–
2	2.8656	3.0366	51.5546	154.7238	−6.8859	–	–	–
3	2.8497	3.1642	57.5076	157.9529	5.6230	36.9750	–	–
4	2.8043	3.5218	33.1138	124.4998	69.1437	64.4481	−5.0075	–
5	2.7925	3.4857	42.2523	122.7959	48.5093	53.7782	16.5547	47.2096

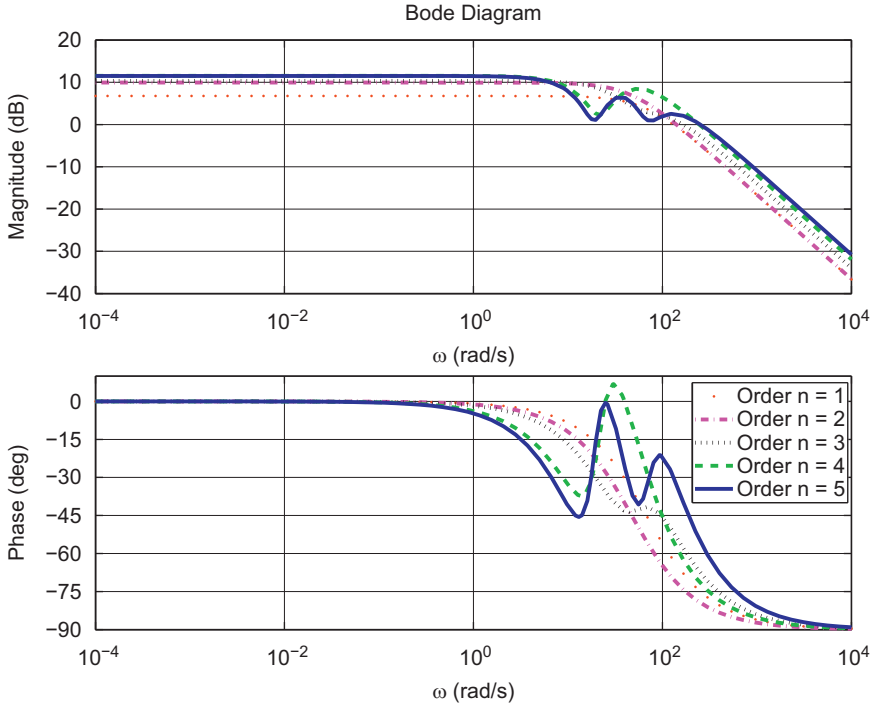

Fig. 5. Bode diagrams of variable-order SPR controllers, $n=1$–5.

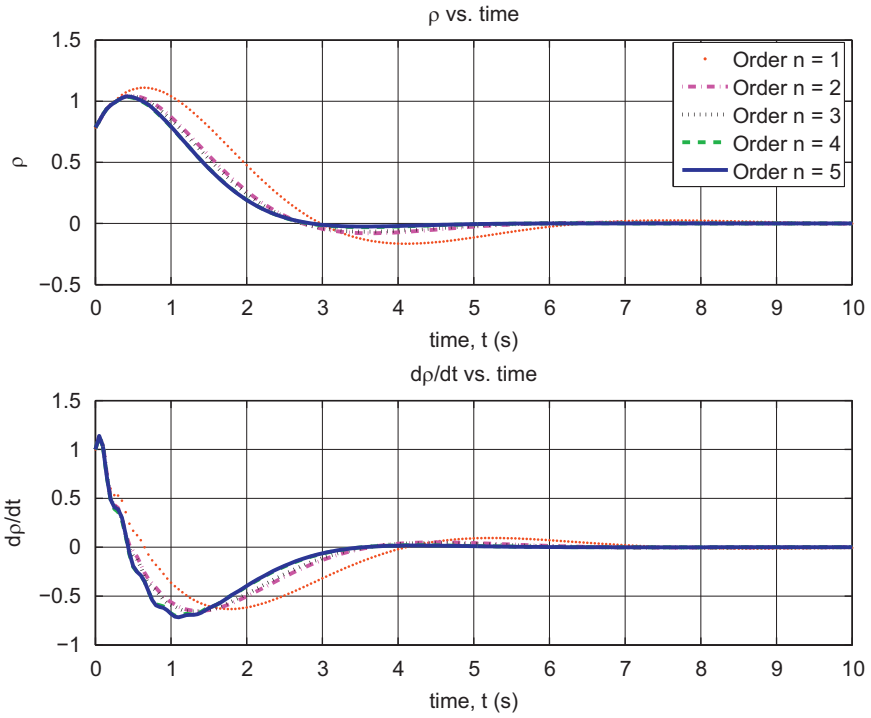

Fig. 6. System responses using variable-order SPR controllers.

Note that as the controller order is increased from $n = 1$ to 3,4,5, the gain and phase of the $n = 3,4,5$ controllers start to take on a similar shape. This can be attributed to the controllers attempting to dampen the higher order modes of the flexible structure. From Fig. 6, it can also be seen that some sort of "law of diminishing returns" is coming into effect. The system response as controlled by the $n=4$ and $n=5$ order controllers is almost identical. Note, the order of the controller is less than the order of the plant being controlled (the plant has an order of six).

Comparing the results of our first controller parameterization discussed in Section 5.1 (i.e., the controller in Eq. (5)) to the present parameterization (i.e., the controller in Eq. (6)), we see that the controller frequency response presented in Fig. 2 is not all that different than the controller frequency responses presented in Fig. 5. The DC gain of each controller is approximately 10 dB, and each controller begins to roll off above 100 rad/s. These characteristics indicate that each controller has converged to a similar minimum. Clearly, however, they have not converged to the same (local) minimum because the frequency responses of the controllers are not identical. The major difference between the two controllers is the gain and phase response between 1 and 100 rad/s. The controller in Fig. 2 has a gain and phase response that changes only a moderate amount compared to the gain and phase responses of the $n = 3, 4, 5$ controllers in Fig. 5. This difference is most likely manifested in the different amount of overshoot seen in Figs. 3 and 6. The system controlled by the controller given in Eq. (5) has more overshoot and a longer settling time than the system controlled by the Ritz controller given in Eq. (6). This indicates that having a rich controller parameterization is better. Similarly, if we compare the objective

function values, we see that the variable controllers of order four and five yield objective function values that are reduced more than the controller of Section 5.1. Again, this indicates that having a richer controller parameterization is better.

5.3. Full-order SPR controller with state–space constraints

In the previous optimization formulations, the SPR controllers were presented and parameterized in the form of transfer functions. It is possible to describe the controller we wish to optimize in a state–space form. Naturally, a different controller parameterization should be developed in order to exploit the unique characteristics of an SPR controller in state–space form.

Recall that the single-link flexible manipulator can be represented in the state–space form of Eq. (5). We would like to design an SPR controller of the form

$$\dot{\mathbf{x}}_c = \underbrace{(\mathbf{A}-\mathbf{B}_2\mathbf{K}_c)}_{\mathbf{A}_c}\mathbf{x}_c + \underbrace{\mathbf{K}_e}_{\mathbf{B}_c}\mathbf{y}$$

$$\mathbf{u} = -\underbrace{\mathbf{K}_c}_{\mathbf{C}_c}\mathbf{x}_c \tag{7}$$

Note, this controller is not an observer-based one. In order to design an SPR controller we must somehow design $\mathbf{K}_c$ and $\mathbf{K}_e$. Let us consider the design of $\mathbf{K}_c$ first. From $\mathcal{H}_2$-control theory, recall the optimal regulator formulation (i.e., the Linear Quadratic Regulator (LQR) formulation): given the weighting matrices $\mathbf{Q}=\mathbf{Q}^{\mathsf{T}}>\mathbf{0}$ and $\mathbf{R}=\mathbf{R}^{\mathsf{T}}>\mathbf{0}$, optimal state feedback of the form

$$\mathbf{u} = -\mathbf{K}_c\mathbf{x}_c$$

can be found via

$$\mathbf{K}_c = \mathbf{R}^{-1}\mathbf{B}_2^{\mathsf{T}}\mathbf{X}$$

by solving the Algebraic Riccati equation for $\mathbf{X}$. In the traditional $\mathcal{H}_2$-optimal control formulation the matrices $\mathbf{Q}$ and $\mathbf{R}$ are specifically defined, however we will parameterize $\mathbf{Q}$ and $\mathbf{R}$ in order to design $\mathbf{K}_c$ to be part of an optimal SPR controller. For simplicity we will specify $\mathbf{Q}$ and $\mathbf{R}$ to be diagonal, that is diag{$\mathbf{Q}$} and diag{$\mathbf{R}$}, where the diagonal elements are design variables in the optimization process. Note that in the SISO case, diag{$\mathbf{R}$} is one variable, r.

With a design strategy for $\mathbf{K}_c$ found, $\mathbf{K}_e$ should be designed to render the controller in Eq. (7) SPR. Recall the definition of an SPR controller in state–space form (Definition 2.2): a controller of the form presented in Eq. (7) is SPR if it is controllable, observable, all eigenvalues of $\mathbf{A}_c$ have real parts less than zero and matrices $\mathbf{P}_c$ and $\mathbf{Q}_c$ can be found which satisfy Eqs. (1a) and (1b). We have already specified $\mathbf{C}_c=\mathbf{K}_c$ and $\mathbf{A}_c=\mathbf{A}-\mathbf{B}_2\mathbf{K}_c$. Given $\mathbf{Q}_c>\mathbf{0}$, $\mathbf{B}_c$, which is equivalent to $\mathbf{K}_e$, may be found by first solving the Lyapunov equation in Eq. (1a) for $\mathbf{P}_c$, then solving Eq. (1b) for $\mathbf{B}_c$. As a result, the controller in Eq. (7) will be SPR. For simplicity, $\mathbf{Q}_c>\mathbf{0}$ will be restricted to be diagonal during the optimization process.

Note that in the previous optimization formulations, the order of controllers that successfully stabilized the plant were all less than the order plant itself. Using the above controller form and parameterization, the order of the controller is equal to that of the

plant. This form of SPR controller is comparable to that of an $\mathcal{H}_2$-optimal controller, but it is not an observer-based compensator.

Given the state–space SISO controller parameterization, the numerical optimization problem is posed as follows:

Design variables: $\mathbf{x} = [\text{diag}\{\mathbf{Q}\}\ r\ \text{diag}\{\mathbf{Q}_c\}\ K_p]$;

Constraints: $\text{diag}\{\mathbf{Q}\} > 0\ ,\ r > 0\ ,\ \text{diag}\{\mathbf{Q}_c\} > 0\ ,\ K_p > 0$;

Objective function: Closed-loop $\mathcal{H}_2$-norm: $\mathcal{J}_2 = \sqrt{\text{tr}\ \mathbf{B}_{zw}^{\mathsf{T}}\mathbf{P}\mathbf{B}_{zw}}$.

5.3.1. Optimization results

The objective function was minimized to a value of $\mathcal{J}_2 = 2.8049$. The convergence tolerance was set to 1×10^{-8}. Shown in Fig. 7 is the Bode diagram of the optimized state–space SPR controller. Following in Fig. 8 is the system response as controlled using the optimized SPR controller.

In Fig. 7 we can clearly see a rather large change in gain and phase just below 100 rad/s. The controller is attempting to dampen the higher order mode of the flexible link. If we compare the controllers from Sections 5.1 and 5.2 to the controller optimized in this section, we see some similarities. Again, the DC gain of each controller is approximately 10 dB, and each controller rolls off after 100 rad/s. The controller frequency response shown in Fig. 7 is similar to that of Fig. 5 (for the $n = 3, 4, 5$ cases) in that the gain and phase of the controllers change somewhat aggressively. This gain and phase change can be attributed to damping the higher frequency modes of the flexible structure.

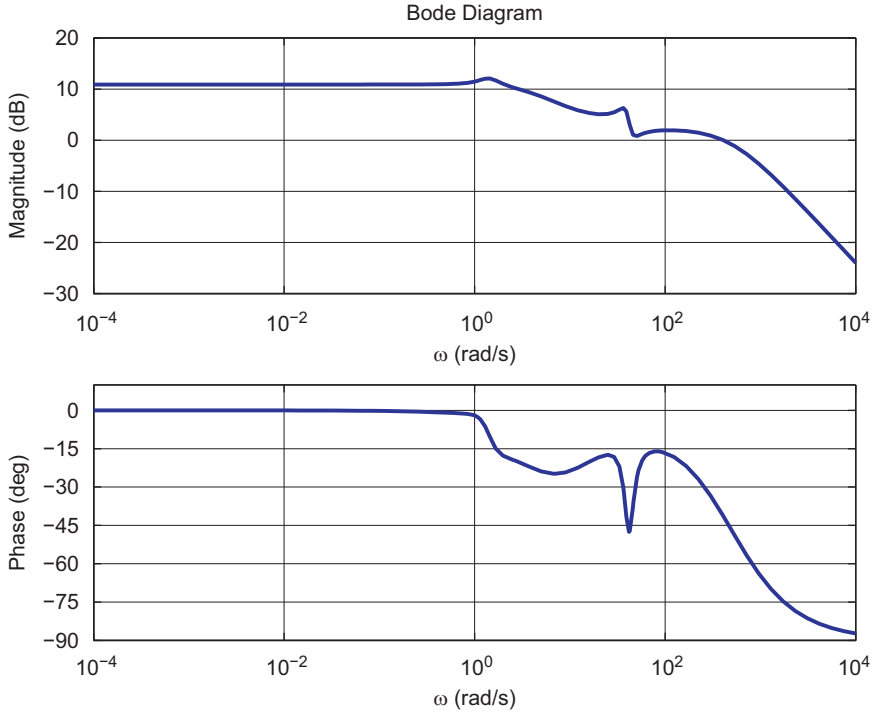

Fig. 7. Bode diagram of state–space SISO SPR controller.

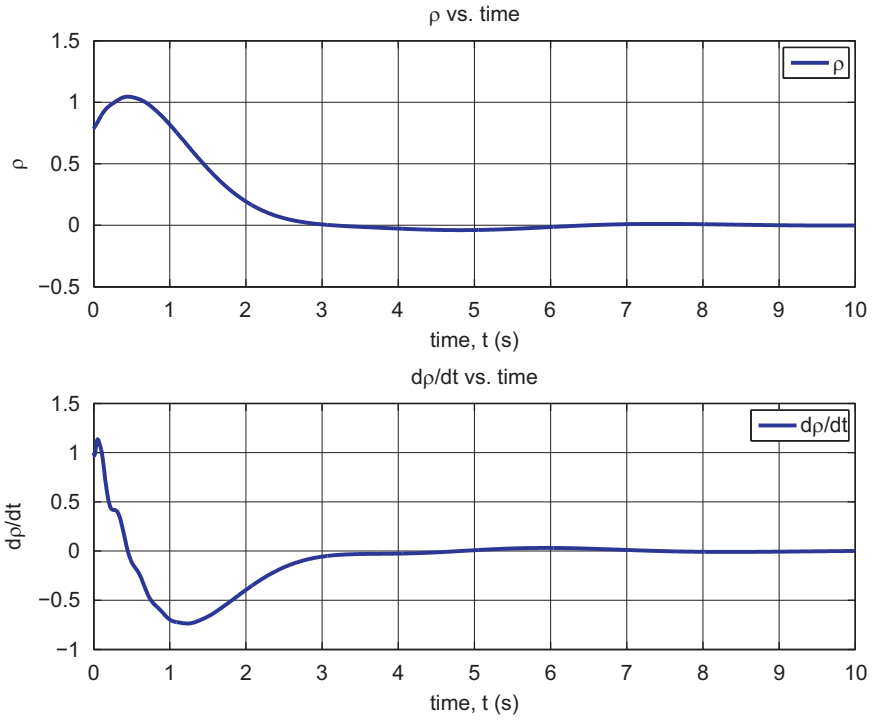

Fig. 8. System response using state–space SISO SPR controller.

6. Optimization of MIMO SPR controllers to control a two-link flexible manipulator

Previously in Section 5 three different SISO SPR controller parameterizations, along with the corresponding SPR constraints were developed. In this section we would like to extend the optimization formulations to MIMO systems, to control the nonlinear two-link flexible manipulator previously discussed. All two-link manipulator simulations presented in the following section will adhere to the following joint trajectory: the initial position and velocity of the tip is $\boldsymbol{\rho}_{\mu=1}=[1,0]^{\mathsf{T}}$ m and $\dot{\boldsymbol{\rho}}_{\mu=1}=[0,0]^{\mathsf{T}}$ m/s. The final position and velocity of the tip is $\boldsymbol{\rho}_{\mu=1}=[0.8365,-0.4830]^{\mathsf{T}}$ m and $\dot{\boldsymbol{\rho}}_{\mu=1}=[0,0]^{\mathsf{T}}$ m/s. This motion corresponds to initial joint angle of $\boldsymbol{\theta}_a=[0^\circ,0^\circ]^{\mathsf{T}}$ and final joint angles of $\boldsymbol{\theta}_b=[-15^\circ,-30^\circ]^{\mathsf{T}}$. Linearization of the two-link manipulator dynamics is about $\boldsymbol{\theta}_b$. The physical values of the two-link manipulator link lengths, link masses, tip-masses, etc. used during optimization and simulation are given in Table 3.

6.1. Diagonal-decoupled SPR controller with deterministic constraints

We will start by constructing a very simple controller composed of third-order transfer functions:

$$\mathbf{G}(s)=\mathbf{C}_c(s\mathbf{I}-\mathbf{A}_c)^{-1}\mathbf{B}_c=\begin{bmatrix}\dfrac{n_{2,11}s^2+n_{1,11}s+n_{0,11}}{s^3+a_{11}s^2+b_{11}s+c_{11}} & 0\\ 0 & \dfrac{n_{2,22}s^2+n_{1,22}s+n_{0,22}}{s^3+a_{22}s^2+b_{22}s+c_{22}}\end{bmatrix} \tag{8}$$

Table 3
Two-link manipulator physical properties.

Length	L_1, L_2	0.5 (m)
Link mass	m_1, m_2	0.3375 (kg)
Modulus of elasticity	E_1, E_2	70×10^9 (Pa)
Link height	h_1, h_2	50 (mm)
Link base width	w_1, w_2	4 (mm)
Link second moment of area	$I_1 = I_2 = \frac{1}{12}hw^3$	5.2083×10^{-10} (m^4)
Link 1 payload mass (Motor 2)	$m_{tip,1}$	0.5 (kg)
Link 1 payload inertia	$J_{tip,1}$	5×10^{-4} (kg m^2)
Link 2 payload mass	$m_{tip,2}$	2.5 (kg)
Link 2 payload inertia	$J_{tip,2}$	2.5×10^{-3} (kg m^2)

This controller is a diagonal-decoupled controller; the two control outputs u_1 and u_2 are not affected by the inputs y_2 and y_1, respectively. A similar controller to the one above was used in Forbes and Damaren [26], however, in Forbes and Damaren [26] the poles of each transfer function were shared.

As in Section 5.1, we will employ the simple parameterization proposed Marquez and Damaren [22]. The controller will be SPR if the two transfer functions within $\mathbf{G}(s)$ are SPR independently. Strictly positive realness of the transfer functions is guaranteed if the denominator polynomials are Hurwitz, and the numerator polynomial coefficients satisfy

$$n_{2,ii} = \frac{b_{ii}c_{ii}k_{1,ii} + c_{ii}k_{2,ii} + a_{ii}k_{3,ii}}{a_{ii}b_{ii}c_{ii} - c_{ii}^2}, \quad n_{1,ii} = \frac{c^2k_{1,ii} + a_{ii}c_{ii}k_{2,ii} + a_{ii}^2k_{3,ii}}{a_{ii}b_{ii}c_{ii} - c_{ii}^2}, \quad n_{0,ii} = \frac{k_{3,ii}}{c_{ii}}$$

where the parameters $k_{1,ii}$, $k_{2,ii}$ and $k_{3,ii}$ satisfy

$$k_{1,ii} \geq 0, \quad k_{2,ii} > -2\sqrt{k_{1,ii}k_{3,ii}}, \quad k_{3,ii} > 0, \quad i = 1,2$$

Given the above MIMO controller form and parameterization, the numerical optimization problem is posed as follows:

Design variables: $\mathbf{x} = [a_{11}\ b_{11}\ c_{11}\ a_{22}\ b_{22}\ c_{22}\ k_{1,11}\ k_{2,11}\ k_{3,11}\ k_{1,22}\ k_{2,22}\ k_{3,22}\ K_{p,11}\ K_{p,12} = K_{p,21}\ K_{p,22}]$;

Constraints: $Re\{\lambda_j(\mathbf{A}_c)\} < 0$ for $j = 1, \ldots, n$, $k_{1,ii} \geq 0$, $k_{2,ii} > -2\sqrt{k_{1,ii}k_{3,ii}}$, $k_{3,ii} > 0$ for $i = 1,2$, $\mathbf{K}_p = \mathbf{K}_p^{\mathsf{T}} > \mathbf{0}$;

Objective function: Closed-loop $\mathcal{H}_2$-norm: $\mathcal{J}_2 = \sqrt{\text{tr } \mathbf{B}_{zw}^{\mathsf{T}}\mathbf{P}\mathbf{B}_{zw}}$.

6.1.1. Optimization results

The objective function was minimized to a value of $\mathcal{J}_2 = 5538.3361$. The convergence tolerance was set to 1×10^{-5}. In Fig. 10 the system response while implementing feedforward and feedback control is shown. The frequency response of the controller transfer matrix $\mathbf{G}(j\omega)$ is shown in Fig. 9. The maximum singular value of $\mathbf{G}(j\omega)$ versus frequency is plotted in the upper part of Fig. 9, $\sqrt{\overline{\lambda}\{\mathbf{G}^{\mathsf{T}}(-j\omega)\mathbf{G}(j\omega)\}}$ where $\overline{\lambda}(\cdot)$ is the maximum eigenvalue. The minimum Hermitian part of $\mathbf{G}(j\omega)$ versus frequency is plotted in the lower part of Fig. 9, $\frac{1}{2}\underline{\lambda}\{\mathbf{G}^{\mathsf{T}}(-j\omega) + \mathbf{G}(j\omega)\}$ where $\underline{\lambda}(\cdot)$ is the minimum eigenvalue. The maximum singular value of the transfer matrix is representative of gain. For an SPR transfer matrix, the minimum Hermitian part must be strictly positive. As such, singular

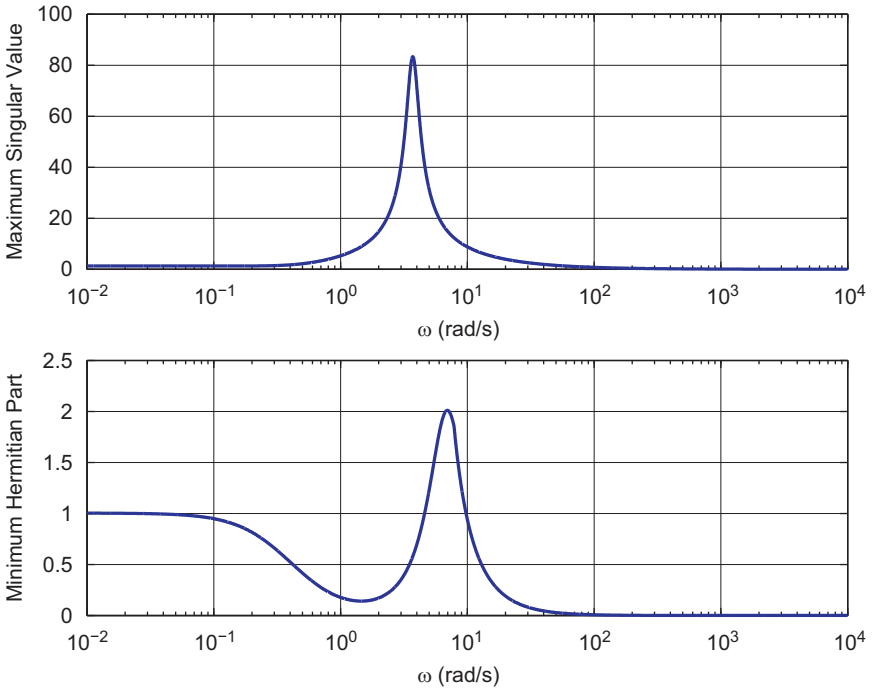

Fig. 9. Diagonal-decoupled SPR controller frequency response.

value and minimum Hermitian part plots provide a graphical means to quickly assess gain and the SPR nature of $\mathbf{G}(j\omega)$, and in a way are an MIMO version of Bode diagrams.

The frequency response of the controller $\mathbf{G}(s)$ is rather simple; the controller adds damping at approximately 4 rad/s. The system response is satisfactory, although there is a residual vibration in the x direction of the manipulator (as shown in the velocity plot of Fig. 10), which is undesirable.

6.2. Variable-order MIMO SPR controller with frequency domain constraints

Consider the following transfer matrix:

$$\mathbf{G}(s) = \mathbf{C}_c(s\mathbf{I}-\mathbf{A}_c)^{-1}\mathbf{B}_c = \underbrace{\left(\sum_{n=1}^{N} h_n \frac{(s-a)^{n-1}}{(s+a)^n}\right)}_{g(s)}\mathbf{Z}$$

where

$$\mathbf{Z} = \mathbf{Z}^{\mathsf{T}} = \begin{bmatrix} Z_{11} & Z_{12} \\ Z_{21} & Z_{22} \end{bmatrix} > \mathbf{0}$$

The above transfer matrix will be SPR provided $g(s)$ is SPR and $\mathbf{Z}$ remains positive definite. The controller will be optimized in the same manner as the controller optimization presented in Section 5.2, stopping when the order of the denominator polynomial of $g(s)$ is five.

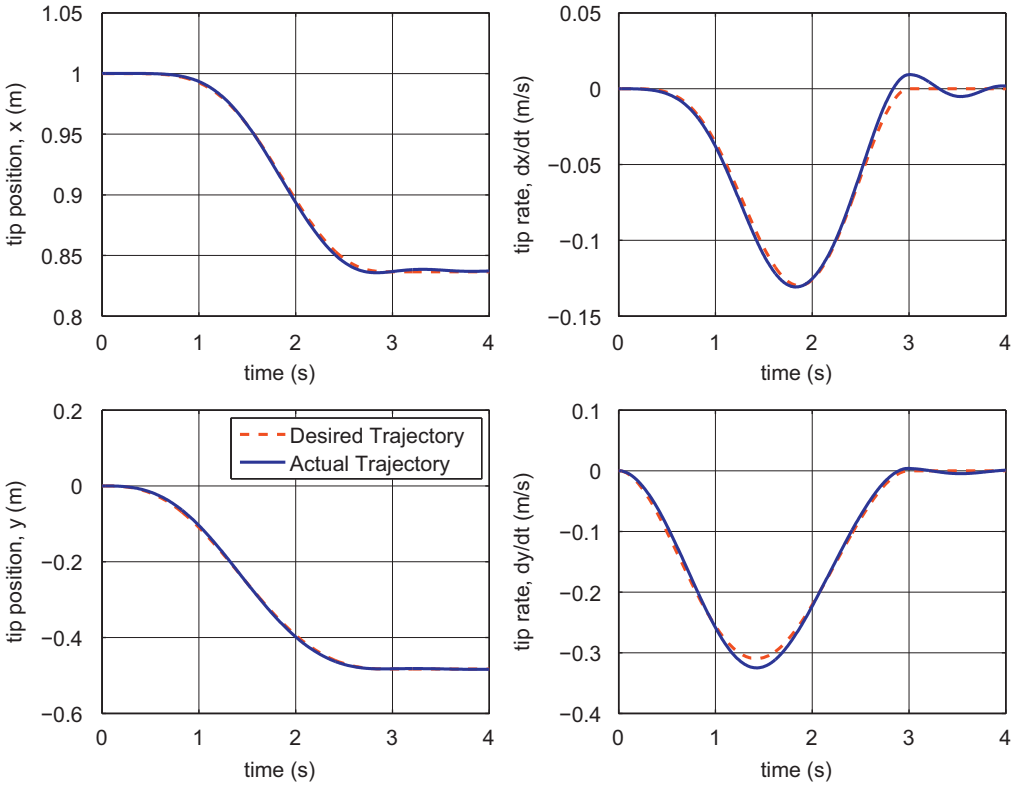

Fig. 10. Two-link flexible manipulator system response as controlled via diagonal-decoupled SPR controller.

Given the above MIMO controller form and parameterization above, the numerical optimization problem is posed as follows:

Design variables: $\mathbf{x} = [a\ h_1\ h_2\ h_3\ h_4\ h_5\ Z_{11}\ Z_{12}\ Z_{22}\ K_{p,11}\ K_{p,12}\ K_{p,22}]$;

Constraints: $Re\{\lambda_j(\mathbf{A}_c)\} < 0 \quad \text{for} \quad j = 1, \ldots, n, \quad Re\{g(j\omega)\} > 0\ \forall \omega \in (0, \infty), \quad \mathbf{Z} = \mathbf{Z}^{\mathsf{T}} > \mathbf{0}, \ \mathbf{K}_p = \mathbf{K}_p^{\mathsf{T}} > \mathbf{0}$;

Objective function: Closed-loop $\mathcal{H}_2$-norm: $\mathcal{J}_2 = \sqrt{\text{tr}\ \mathbf{B}_{zw}^{\mathsf{T}} \mathbf{P} \mathbf{B}_{zw}}$.

6.2.1. Optimization results

The objective function was minimized to a value of $\mathcal{J}_2 = 99.0982$. The convergence tolerance was set to 1×10^{-8}. The values of the objective function and the parameter values a and h_n as n is increased from one to five are listed in Table 4. The frequency response of $\mathbf{G}(s)$ is shown in Fig. 11. The system response of the two-link manipulator is shown in Fig. 12.

In Table 4, notice that the objective function steadily decreases from $\mathcal{J}_2 = 166.2870$ to 99.0982 as n is increased from one to five. This informs us that a higher order controller is more effective at minimizing the closed-loop $\mathcal{H}_2$-norm. Also notice that as the manipulator comes to its final set-point there is a some overshoot in both the x and y directions, but then the manipulator gently stops moving, and there is a very little residual vibration of the

Table 4
Variable-order MIMO SPR controller optimization evolution.

n	$\mathcal{J}_2$	a	h_1	h_2	h_3	h_4	h_5
1	166.2870	104.4510	124.5664	–	–	–	–
2	143.5452	105.7637	124.4330	31.9724	–	–	–
3	136.0341	105.4809	137.5570	59.7808	2.1758	–	–
4	105.7945	105.4107	121.6304	47.2990	70.6868	62.5926	–
5	99.0982	105.4056	122.2541	49.1886	72.1574	60.6160	31.1785

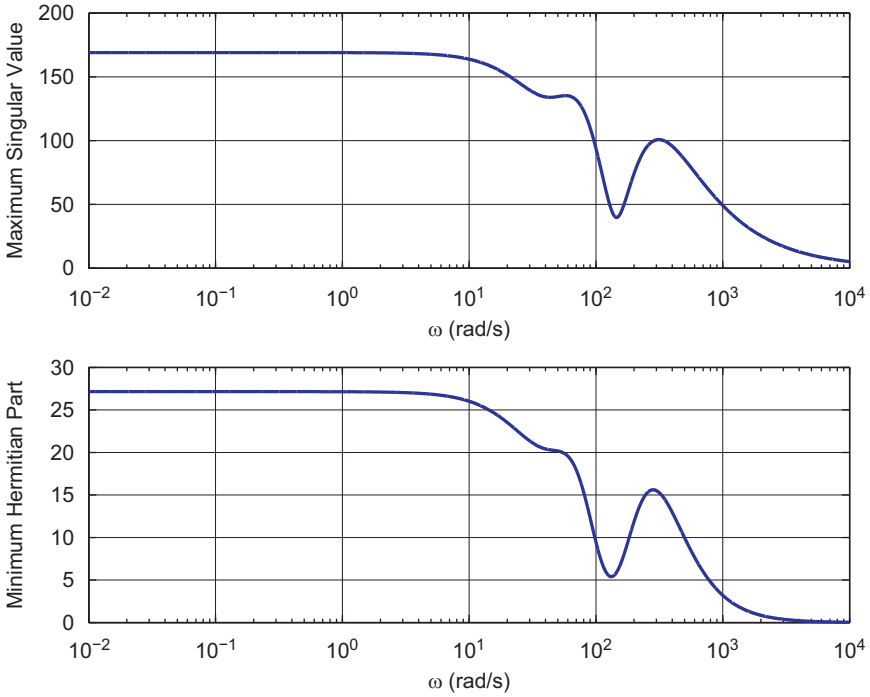

Fig. 11. Iterative SPR controller frequency response.

manipulator tip. This controller performs better than the diagonal-decoupled controller developed in Section 6.1.

If we compare the frequency responses of the diagonal-decoupled SPR controller of Section 6.1 and the variable-order SPR controller developed in this section, they are not similar. The gain of the variable-order SPR controller is quite high at low frequency, unlike the diagonal-decoupled controller. Additionally, the variable-order SPR controller has high frequency dynamics that are active, while the diagonal-decoupled SPR controller has rolled off. The simple diagonal-decoupled SPR controller, although optimal given the parameterization, has reach a local optimum within the design space. On the other hand, the variable-order SPR controller has found a "better" local optimum owing to its richer parameterization. In general, having a higher order and richer parameterization is better.

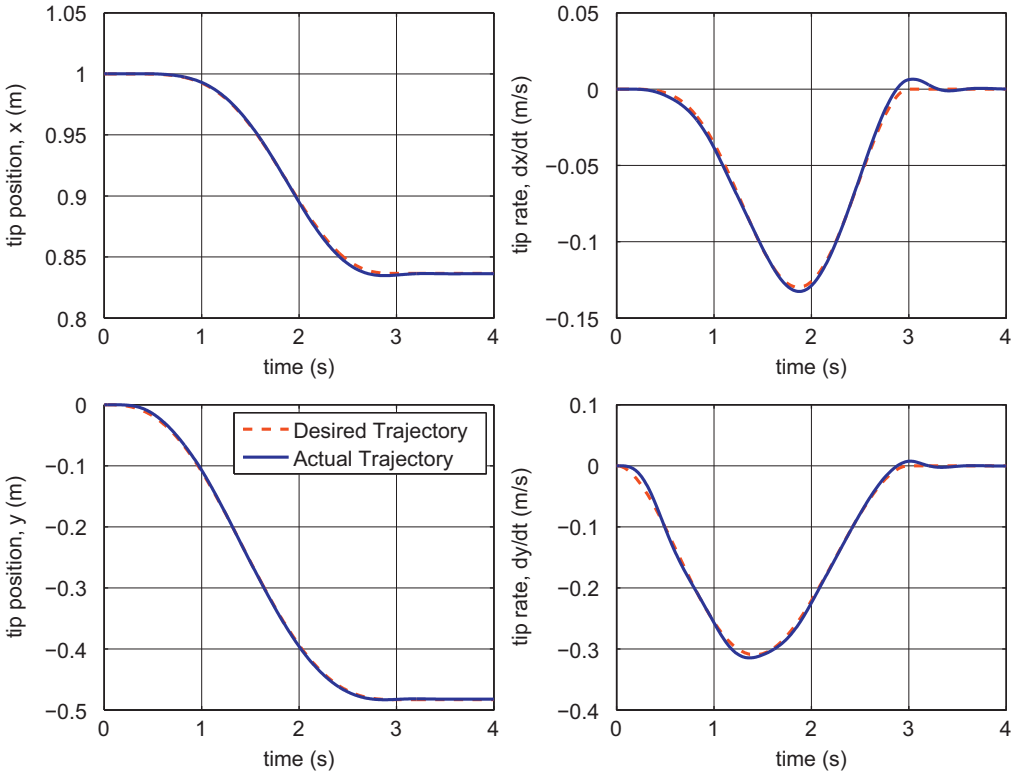

Fig. 12. Two-link flexible manipulator system response as controlled via variable-order MIMO SPR controller.

6.3. Full-order MIMO SPR controller with state–space constraints

The previous MIMO optimization formulations have relied heavily on the form and parameterization of transfer functions used to create transfer matrices. As in Section 5.3, it is possible to formulate the MIMO controller optimization problem using a state–space controller form and appropriate parameterization.

Recall that the nonlinear two-link flexible manipulator differential equations can be linearized and expressed in the state–space form of Eq. (4). We would like to design an MIMO SPR controller of the form presented in Eq. (7). We will use the procedure presented in Section 5.3 to create $\mathbf{K}_c$ and $\mathbf{K}_e$ such that the controller is SPR. We refer to this controller as a *full-order* controller because, unlike the previous optimization formulations, the controller we seek to optimize and the linearized plant have the same number of states. Recall that this controller is not observer-based.

Given the state–space MIMO controller parameterization, the numerical optimization problem is posed as follows:

Design variables: $\mathbf{x} = [\text{diag}\{\mathbf{Q}\}\ \text{diag}\{\mathbf{R}\}\ \text{diag}\{\mathbf{Q}_c\}\ K_{p,11}\ K_{p,12}\ K_{p,22}]$;

Constraints: $\text{diag}\{\mathbf{Q}\} > 0$, $\text{diag}\{\mathbf{R}\} > 0$, $\text{diag}\{\mathbf{Q}_c\} > 0$, $\mathbf{K}_p = \mathbf{K}_p^{\mathsf{T}} > \mathbf{0}$;

Objective function: Closed-loop $\mathcal{H}_2$-norm; $\mathcal{J}_2 = \sqrt{\text{tr}\ \mathbf{B}_{zw}^{\mathsf{T}} \mathbf{P} \mathbf{B}_{zw}}$.

6.3.1. Optimization results

The objective function was minimized to a value of $\mathcal{J}_2 = 80.9141$. The convergence tolerance was set to 1×10^{-8}. The frequency response of the controller $\mathbf{G}(s)$ created via the state–space parameterization and optimization is shown in Fig. 13. Shown in Fig. 14 is the system response of the two-link manipulator.

The frequency response of the full-order SPR controller is quite interesting. Notice that the gain is high, but not as high as, for example, the variable-order SPR controller gain in Fig. 11. Also, note that the full-order SPR controller begins to roll off above 10^4 rad/s, unlike both the diagonal-decoupled (Section 6.1) and variable-order SPR controllers.

The performance of the closed-loop system as controlled by the full-order SPR controller is quite good. There is only a moderate amount of overshoot at the end of the manipulator maneuver, with no residual vibration. The full-order SPR controller outperforms the diagonal-decoupled SPR controller significantly. However, the performance of the variable-order and full-order SPR controller is essentially the same.

Recall that each controller parameterization is used within an optimization scheme that minimized the closed-loop $\mathcal{H}_2$-norm given a particular set of weights (i.e., the $\mathbf{B}_1$, $\mathbf{C}_1$, $\mathbf{D}_{12}$, $\mathbf{D}_{21}$ matrices). Interestingly, the present parameterization is able to attain a smaller closed-loop $\mathcal{H}_2$-norm as compared to the diagonal-decoupled and variable-order parameterizations. This is due to the fact that the full-order parameterization allows for controllers that are of greater order (compared to the other parameterizations).

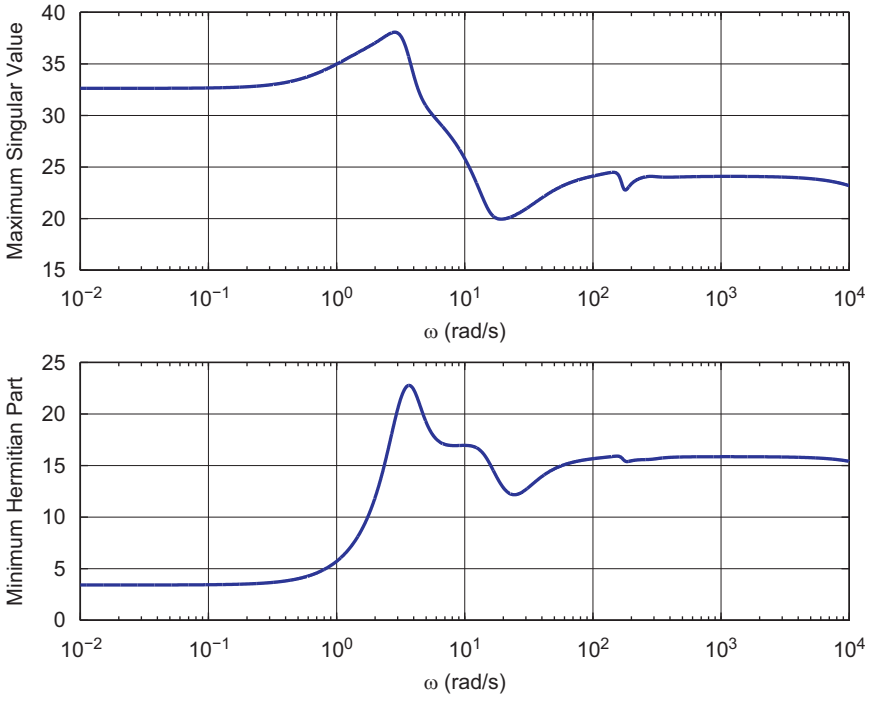

Fig. 13. Full-order SPR controller frequency response.

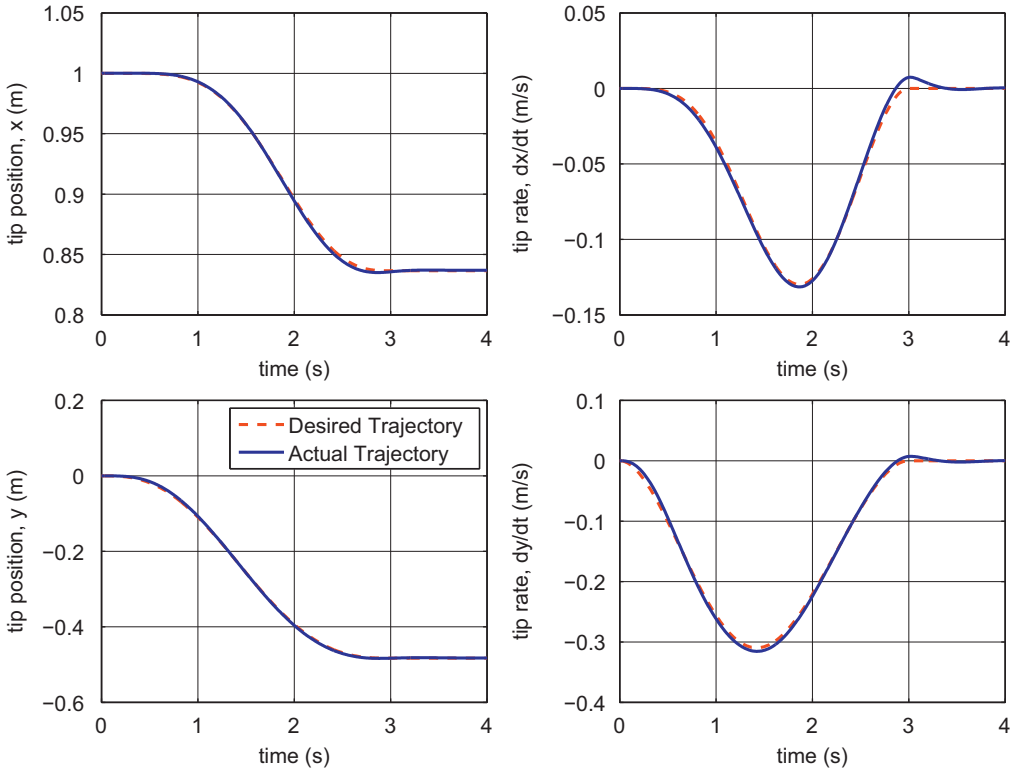

Fig. 14. Two-link flexible manipulator system response as controlled via SPR controller parameterized using state–space techniques.

7. Discussion and closing remarks

In this paper, we have presented various SPR controller parameterizations to be used within a numerical optimization setting. Our optimization objective function is to minimize the closed-loop $\mathcal{H}_2$-norm of the system while varying design variables associated with an SPR controller. The constraints ensuring SPRness are parameterization dependent. We use the optimized SPR controller to control single- and two-link flexible manipulators.

The first SISO controller parameterization involved a simple third-order transfer function as the controller (Section 5.1). The form of the transfer function allowed the results of Marquez and Damaren [22] to be used to enforce SPRness. In the second SISO controller parameterization (Section 5.2) a variable-order controller was optimized between order one and order five. Frequency domain constraints ensured that the controller would be SPR. The third SISO controller parameterization tackled SPR controller design using the controllers state–space matrices (Section 5.3). Simple constraints on three weighting matrices along with the KYP Lemma ensured the controller be SPR. All the optimization results were successful with respect to finding an optimal SISO SPR controller. All formulations produced good closed-loop system responses. The closed-loop $\mathcal{H}_2$-norm using the optimized SPR controllers was all very close, in the range of $\mathcal{J}_2 = 2.8$. This tells us that the three controller parameterizations are almost all equal with respect to finding the global optimum for an SPR controller.

The first MIMO controller optimized consists of two decoupled controllers (Section 6.1). The second MIMO controller considered consisted of a variable-order SPR transfer function times a positive definite matrix (Section 6.2). The last MIMO formulation utilized the state–space form of a controller along with the KYP Lemma to enforce the SPR constraint (Section 6.3). The controller parameterization that led to the lowest value of the objective function was the full-order formulation (Section 6.3). The objective function was minimized to a value of $\mathcal{J}_2 = 80.9141$, as compared to $\mathcal{J}_2 = 5538.3361$ for the diagonal-decoupled controller, and $\mathcal{J}_2 = 99.0982$ for the variable-order controller. These results can be explained via the number of design variables; the state–space parameterization is the richest, having a design space with a greater number of design variables to be used during the quest to find an optimal SPR controller. Also, considering that the diagonal-decoupled controller could only minimize the closed-loop $\mathcal{H}_2$-norm to a value two orders of magnitude greater than both the variable-order and full-order controller, it is evident that parameterization is just not rich enough. In particular, having a diagonal structure is not ideal, as the plant being controlled is not decoupled. To summarize, within a numerical optimization the controller parameterization should be rich.

As mentioned in the Introduction, finding optimal SPR controllers is a worthwhile pursuit in the context of passivity-based control. The majority of the formulations in the literature yield controllers which are observer-based, and of the same order as the plant [5–9]. In our work we have explored various controller parameterizations that can be used within an optimization framework to find optimal SPR controllers. In particular, our contributions are (1) the parameterizations themselves, along with the associated constraints (in both SISO and MIMO forms), (2) clearly showing that SPR controllers that are not observer-based can effectively control interesting systems such as flexible manipulators, and (3) showing (through numerical studies) that richer controller parameterizations are more effective at minimizing the closed-loop $\mathcal{H}_2$-norm (our performance criteria). Indeed, we have not definitively shown that (through a proof, for example) the optimal SPR controller that solves the $\mathcal{H}_2$ control problem is observer-based, but the evidence put forth in this paper suggests that an optimal SPR controller does not have to be observer-based. Similarly, we have not definitively shown that the controllers should have the same order as the plant, however it seems that the controller parameterization should be very rich, and have an order very close to the order of the plant.

In conclusion, the development and exploration of controller parameterizations to be used within a numerical optimization setting where the closed-loop $\mathcal{H}_2$-norm is minimized has been interesting. Although the plants controlled in this paper were robotic systems, the formulations presented in this paper can be applied to any passive/PR plant. In the future we will explore other optimization objective functions and constraints, such as the minimization of the closed-loop $\mathcal{H}_\infty$-norm subject to the constraint that the compensator must be SPR.

References

[1] C.A. Desoer, M. Vidyasagar, Feedback Systems: Input–Output Properties, Academic Press, New York, NY, 1975.

[2] C.J. Damaren, Passivity and noncollocation in the control of flexible multibody systems, Journal of Dynamic Systems, Measurement and Control 122 (1) (2000) 11–17.

[3] J.T. Wen, Time domain and frequency domain conditions for strict positive realness, IEEE Transactions on Automatic Control 33 (10) (1988) 988–992.

[4] R.J. Benhabib, R.P. Iwens, R.L. Jackson, Stability of large space structure control systems using positivity concepts, Journal of Guidance, Control, and Dynamics 4 (5) (1981) 487–494.
[5] M.D. McLaren, G.L. Slater, Robust multivariable control of large space structures using positivity, Journal of Guidance, Control, and Dynamics 10 (4) (1987) 393–400.
[6] R. Lozano-Leal, S. Joshi, On the design of dissipative LQG-type controllers, Proceedings of the 27th IEEE Decision and Control Conference, 1988, pp. 1645–1646.
[7] W.M. Haddad, D.S. Bernstein, Y.W. Wang, Dissipative H_2/H_∞ controller synthesis, IEEE Transaction on Automatic Control 30 (4) (1994) 827–831.
[8] J.C. Germoel, P.B. Gapsik, Synthisis of positive real $\mathcal{H}_2$ controllers, IEEE Transactions on Automatic Control 42 (7) (1997) 988–992.
[9] T. Shimomura, S.P. Pullen, Strictly positive real $\mathcal{H}_2$ controller synthesis via iterative algorithms for convex optimization, Journal of Guidance, Control and Dynamics 25 (6) (2002) 1003–1011.
[10] C.J. Damaren, Optimal strictly positive real controllers using direct optimization, Journal of the Franklin Institute 343 (2006) 271–278.
[11] C.J. Damaren, H.J. Marquez, A.G. Buckley, Optimal strictly positive real approximations for stable transfer functions, IEE Proceedings – Control Theory and Applications 143 (6) (1996) 537–542.
[12] D. Henrion, Linear matrix inequalities for robust strictly positive real design, IEEE Transaction on Circuits and Systems 49 (7) (2002) 1017–1020.
[13] G. Tao, P. Ioannou, Frequency domain conditions for strictly positive real functions, IEEE Transactions on Automatic Control 32 (1) (1987) 53–54.
[14] G. Tao, P. Ioannou, Strictly positive real matrices and the Lefschetz–Kalman–Yakubovich lemma, IEEE Transactions on Automatic Control 33 (12) (1988) 1183–1185.
[15] S. Joshi, S. Gupta, On a class of marginally stable positive real systems, IEEE Transactions on Automatic Control 41 (1) (1996) 152–155.
[16] H. Marquez, Nonlinear Control Systems, John Wiley and Sons, Inc., Hoboken, NJ, 2003.
[17] B. Brogliato, R. Lozano, B. Maschke, O. Egeland, Dissipative Systems Analysis and Control: Theory and Applications, second ed, Springer, London, 2007.
[18] C.J. Damaren, I. Sharf, Simulation of flexible-link manipulators with inertial and geometric nonlinearities, Journal of Dynamic Systems, Measurement, and Control 117 (1995) 74–87.
[19] C.J. Damaren, Modal properties and control system design for two-link flexible manipulators, International Journal of Robotics Research 17 (6) (1998) 667–678.
[20] C.J. Damaren, Passivity analysis for flexible multilink space manipulators, Journal of Guidance, Control and Dynamics 18 (2) (1995) 272–279.
[21] J. Nocedal, S.J. Wright, Numerical Optimization, second ed, Springer Science and Business Media, New York, NY, 2006.
[22] H.J. Marquez, C.J. Damaren, On the design of strictly positive real transfer functions, IEEE Transactions on Circuits and Systems 42 (4) (1995) 214–218.
[23] E. Polak, S.E. Salcudean, On the design of linear multivariable feedback systems via constrained nondifferentiable optimization in H_∞ spaces, IEEE Transaction on Automatic Control 34 (3) (1989) 268–276.
[24] Z. Hu, S.E. Salcudean, P.D. Loewen, Numerical solution of the multiple objective control system design problem for SISO systems, Proceedings of the American Control Conference, 1995, pp. 1458–1462.
[25] S.P. Boyd, C.H. Barratt, Linear Controller Design, Limits of Performance, Prentice-Hall, Englewood Cliffs, NJ, 1991.
[26] J.R. Forbes, C.J. Damaren, Design of gain-scheduled strictly positive real controllers using numerical optimization for flexible robotic systems, Journal of Dynamic Systems, Measurement, and Control 132 (3) (2010) 034503 1–7.